Virchows Archiv (2019) 474:585–598
https://doi.org/10.1007/s00428-018-02516-2

ORIGINAL ARTICLE

Targeted sequencing with a customized panel to assess histological typing in endometrial carcinoma

Dolors Cuevas[1] · Joan Valls[1] · Sònia Gatius[1] · Berta Roman-Canal[2] · Elena Estaran[1] · Eduard Dorca[2] · Maria Santacana[1] · Marta Vaquero[1] · Núria Eritja[1] · Ana Velasco[1] · Xavier Matias-Guiu[1,2]

Received: 22 November 2018 / Revised: 19 December 2018 / Accepted: 20 December 2018 / Published online: 1 February 2019

Abstract

The two most frequent types of endometrial cancer (EC) are endometrioid (EEC) and serous carcinomas (SC). Differential diagnosis between them is not always easy. A subset of endometrial cancers shows misleading microscopical features, which cause problems in differential diagnosis, and may be a good scenario for next-generation sequencing. Previous studies have assessed the usefulness of targeted sequencing with panels of generic cancer-associated genes in EC histological typing. Based on the analysis of TCGA (The Cancer Genome Atlas), EEC and SC have different mutational profiles. In this proof of principle study, we have performed targeted sequencing analysis with a customized panel, based on the TCGA mutational profile of EEC and SC, in a series of 24 tumors (16 EEC and 8 SC). Our panel comprised coding and non-coding sequences of the following genes: *ABCC9*, *ARID1A*, *ARID5B*, *ATR*, *BCOR*, *CCND1*, *CDH19*, *CHD4*, *COL11A1*, *CSDE1*, *CSMD3*, *CTCF*, *CTNNB1*, *EP300*, *ERBB2*, *FBXW7*, *FGFR2*, *FOXA2*, *KLLN*, *KMT2B*, *KRAS*, *MAP3K4*, *MKI67*, *NRAS*, *PGAP3*, *PIK3CA*, *PIK3R1*, *PPP2R1A*, *PRPF18*, *PTEN*, *RPL22*, *SCARNA11*, *SIN3A*, *SMARCA4*, *SPOP*, *TAF1*, *TP53*, *TSPYL2*, *USP36*, and *WRAP53*. Targeted sequencing validation by Sanger sequencing and immunohistochemistry was performed in a group of genes. *POLE* mutation status was assessed by Sanger sequencing. The most mutated genes were *PTEN* (93.7%), *ARID1A* (68.7%), *PIK3CA* (50%), and *KMT2B* (43.7%) for EEC, and *TP53* (87.5%), *PIK3CA* (50%), and *PPP2R1A* (25%) for SC. Our panel allowed correct classification of all tumors in the two categories (EEC, SC). Coexistence of mutations in *PTEN*, *ARID1A*, and *KMT2B* was diagnostic of EEC. On the other hand, absence of *PTEN*, *ARID1A*, and *KMT2B* mutations in the presence of *TP53* mutation was diagnostic of SC. This proof of concept study demonstrates the suitability of targeted sequencing with a customized endometrial cancer gene panel as an additional tool for confirming histological typing.

Keywords Endometrial carcinoma · Histological type · Endometrioid · Serous · Biomarker · Targeted sequencing

Introduction

In western countries, endometrial carcinoma (EC) is the most common cancer of the female genital tract. Prognosis is quite good for low-grade, early-stage tumors. However, clinical outcome is not good for some tumor types and advanced-stage tumors. There are different histological types of EC. The two most common types of tumors are endometrioid carcinomas (EEC) and serous carcinomas (SC). Histological typing is a good prognostic indicator in EC [1–4].

Histological classification of EC is easy in the vast majority of cases. However, diagnosis may be difficult in some high-grade tumors, which sometimes show combined or mixed features [5–7]. Furthermore, some EEC may exhibit papillary architecture (characteristic of SC), and also some SC may show a predominant glandular arrangement (typical of EEC). Finally, each of them (EEC or SC) may show a predominant solid pattern. There is a poor inter-observer agreement in assessing histological type in this subset of tumors, even among experts [8].

Immunohistochemistry (IHC) has some value in histological typing. Some immunohistochemical markers, such as p53,

Electronic supplementary material The online version of this article (https://doi.org/10.1007/s00428-018-02516-2) contains supplementary material, which is available to authorized users.

✉ Xavier Matias-Guiu
fjmatiasguiu.lleida.ics@gencat.cat

[1] Hospital Universitari Arnau de Vilanova, Universitat de Lleida, IRBLLEIDA, CIBERONC, Lleida, Spain

[2] Hospital Universitari de Bellvitge, IDIBELL, Barcelona, Spain

p16, PTEN, and ARID1A present a distinct immunostaining pattern between different types of tumors, but there are many exceptions, particularly in high-grade EEC. TCGA performed an integrating genomic, transcriptomic, and proteomic characterization of EC, based on array and sequencing technologies [9]. In this study, the mutation profile of EEC and SC was different. The most frequently mutated genes in EEC were *PTEN* (77.7%), *PIK3CA* (53.1%), *PIK3R1* (37.1%), *CTNNB1* (36.6%), *ARID1A* (35.4%), *KRAS* (24.6%), and *CTCF* (20.6%), while the most frequently mutated genes in SC were *TP53* (90.7%), *PIK3CA* (41.9%), *FBXW7* (30.2%), *PPP2R1A* (36.6%), and *CHD4* (16.3%).

The aim of the study was to check the usefulness of targeted sequencing analysis in assessing histological type in EC. To this purpose, we designed a specific customized gene panel, based on the sequencing profile of EEC and SC, according to TCGA results. The panel was tested in a series of 24 tumors (16 EEC and 8 SC), well characterized at the pathological level.

Materials and methods

Case selection

Twenty four tumors and their corresponding matched normal tissues were selected from the frozen tumor tissue bank of IRBLLEIDA. Sixteen corresponded to EEC and 8 to SC. All tumors were diagnosed at the Department of Pathology of Hospital Arnau de Vilanova of Lleida, by following the most recent World Health Organization (WHO) criteria. They were surgically staged and graded according to the International Federation of Gynecology and Obstetrics (FIGO) staging and grading systems. Table 1 shows the main clinical and pathological features, including the TCGA-based molecular classification of each of them with the surrogate markers (*POLE*, p53, MSH-6, PMS-2). Mean follow up period was 76 months (range 24 to 108). A specific informed consent was used. Matched formalin-fixed, paraffin-embedded tissue blocks were used for immunohistochemical validation.

Samples

For each case, after surgery, tumor and normal tissue were obtained and immediately frozen and stored at − 80 °C at the Tissue Bank of IRBLLEIDA. Tumor and normal tissue quality was assessed in hematoxylin and eosin (H&E) sections. The percentage volume of tumor, necrosis, and non-tumor tissue was quantified in each tissue block. DNA was purified using DNeasy Blood and Tissue Kit (Qiagen) according to manufacturer's instructions. For all samples, DNA purity was determined using a Nanodrop ND-1000 (Thermo Fisher Scientific) and for targeted next-generation sequencing, DNA samples were further quantified using the Qubit dsDNA HS Assay Kit (Invitrogen, Thermo Fisher Scientific), performed on the Qubit Fluorometer 1.0 (Invitrogen, Life Technologies).

Targeted sequencing analysis

Targeted sequencing analysis was performed to detect mutations in 40 genes that have been previously found to be recurrently mutated in endometrial carcinoma by the TCGA [9]. These genes were grouped in seven signaling pathways (Table 2) as cell cycle, chromatin organization, cell-cell communication, Wnt signaling, PI3K/AKT/mTOR signaling, RTK/RAS/MAPK signaling, and diverse which includes genes with different functionalities. Our TruSeq genetic panel design included 1333 amplicons (250 bp in length) that covered 98.59% of exons, introns, and untranslated regions of the selected genes. Custom amplicon library was created using 100 ng of genomic DNA from tumor and non-tumor specimens according to manufacturer's instructions (TruSeq Custom Amplicon (TSCA) library preparation guide). In brief, a custom pool containing specific oligos to targeted regions of interest was hybridized to genomic DNA samples. After removal of unbound oligos, an extension-ligation step was performed. Resulting products were amplified using primers that add multiplexing index sequences for sample tagging as well as common adapters required for cluster generation. Before pooling, normalization was performed by quantifying individual libraries using the Qubit fluorometer and then pooled based on equal concentrations. Pooled TruSeq libraries were sequenced using Miseq Reagent kit v3 600 cycles (Illumina).

Bioinformatic analysis

Bioinformatic analysis was performed by Sistemas Genómicos S.L. (Spain). Sistemas Genómicos (SG) pipeline included fastq files processing, base calling, quality score assignment, read alignment against the human reference genome version GRCh38/hg38, quality control of mapping quality, coverage analysis, variant calling, and variant annotation. After completion of the pipeline, manual inspection of the variant list was performed. With the paired normal-tumor analysis, we selected as potential somatic mutations those variants with a VAF (variant allelic frequency) above 0.15 and a depth above 100 in the tumor tissue and not present in the normal tissue. Somatic gene mutations were further filtered based on the canonical isoforms and the variant effect on the transcript, excluding the non-canonical isoforms and synonymous variants. To

Table 1 Clinical and pathological features, including TCGA-based molecular classification of the tumors by surrogate markers

Case	Age	Histological type	Grade	Stage	Molecular classification	Follow-up
1	86	EEC	II	IB	MSI (hypermutated)	NED
2	91	EEC	III	II	Serous-like	DOD
3	94	EEC	II	IB	MSI (hypermutated)	NED
4	91	EEC	II	IB	NSMP	NED
5	83	EEC	II	IA	NSMP	NED
6	60	EEC	III	IIIA	Double mutated[a]	NED
7	67	EEC	III	IB	Serous-like	NED
8	76	EEC	II	IB	MSI (hypermutated)	NED
9	77	EEC	III	IB	MSI (hypermutated)	NED
10	86	EEC	I	IB	NSMP	NED
11	73	EEC	III	IB	POLE-mutated	NED
12	77	EEC	III	IB	NSMP	NED
13	77	EEC	III	IB	MSI (hypermutated)	NED
14	77	EEC	II	II	NSMP	NED
15	78	EEC	I	IB	NSMP	DDD
16	59	EEC	III	IB	Double mutated[a]	NED
17	86	SC	III	IA	Serous-like	DOD
18	89	SC	III	IIIA	Serous-like	DOD
19	85	SC	III	IB	Serous-like	AWOD
20	76	SC	III	IA	Serous-like	DOD
21	81	SC	III	IA	NSMP	DOD
22	87	SC	III	IIIB	Serous-like	DOD
23	93	SC	III	IB	Serous-like	DOD
24	96	SC	III	II	Serous-like	DOD

[a] Indicates double mutated cases characterized by both p53 "mutated" IHC pattern and MSI. *MSI (hypermutated)*, microsatellite unstable; *NSMP*, tumors with no specific molecular profile; *EEC*, endometrial endometrioid carcinoma; *SC*, serous carcinoma; *NED*, no evidence of disease; *DOD*, dead of disease; *DDD*, dead of different disease; *AWOD*, alive with other disease

restrict the analysis, mutations were also selected based on their frequency on population databases (NHLBI-ESP and 1000 Genomes Project) to discard known variants with a MAF (minor allele frequency) higher than 1%. Lastly, selected somatic variants were categorized into four according to their pathogenicity degree. Pathogenic variant (PV) category included variants previously reported on COSMIC database (Catalog of Somatic Mutations in Cancer), associated with disease and evaluated as deleterious with different pathogenicity predictors (Polyphen2, Sift, Condel, and Fathmm). Likely pathogenic variants (LPV) were variants reported on COSMIC with some evidence of disease association, but with absent data on pathogenicity prediction. Variants of unknown significance (VUS) included variants that had not been previously reported either as a disease associated or as a normal variant, but whose pathogenicity could not be established with certainty. And the likely benign or neutral variants (LBNV) were variants annotated on COSMIC but evaluated as neutral or benign through pathogenicity predictors.

Sanger sequencing validation and *POLE* mutation analysis

A total of 46 variants identified by targeted sequencing analysis were validated by Sanger sequencing. These variants comprise hotspots of the following genes: *TP53*, *PTEN*, and *ARID1A*. We also performed a *POLE* exons 9, 11, 13, and 14 Sanger sequencing analysis in all samples. Sequencing reactions were carried out with BigDye Terminator Kit v3.1 (Applied Biosystems, Thermo Fisher Scientific) and run on Applied Biosystems 3130 Genetic Analyzer (Applied Biosystems).

Immunohistochemistry testing

Formalin-fixed, paraffin-embedded tissue blocks were sectioned at a thickness of 3 μm, dried for 1 h at 65° before pre-treatment procedure of deparaffinization, rehydration, and epitope retrieval in the Pre-Treatment Module, PT-LINK (DAKO) at 95 °C for 20 min in 50×

Table 2 List of the 40 genes included in the customized panel

Gene symbol	Chr.	Gene target (bps)	Gene description	Related pathway
ABCC9	chr12	11,265	ATP binding cassette subfamily C member 9	Cell cycle
ATR	chr3	16,885	ATR serine/threonine kinase	
CCND1	chr11	1689	Cyclin D1	
CSDE1	chr1	421	Cold shock domain containing E1	
EP300	chr22	12,740	E1A binding protein P300	
MKI67	chr10	11,934	Marker of proliferation Ki-67	
PPP2R1A	chr19	4384	Protein Phosphatase 2 scaffold subunit A alpha	
TP53	chr17	3327	Tumors protein P53	
WRAP53	chr17	273	WD repeat containing antisense to TP53	
ARID1A	chr1	10,823	AT-rich interaction domain 1A	Chromatin organization
ARID5B	chr10	6419	AT-rich interaction domain 5B	
CHD4	chr12	12,781	Chromodomain helicase DNA-binding protein 4	
KMT2B	chr19	13,342	Lysine methyltransferase 2B	
SMARCA4	chr19	11,274	SWI/SNF related, matrix associated, actin dependent regulator of chromatin, subfamily A, member 4	
CDH19	chr18	4550	Cadherin 19	Cell-cell communication
COL11A1	chr1	18,812	Collagen type XI alpha 1 chain	
CTNNB1	chr3	5164	Catenin beta 1	WNT signaling
ERBB2	chr17	9822	Erb-B2 receptor tyrosine kinase 2	PI3K/AKT/mTOR signaling
PIK3CA	chr3	7060	Phosphatidylinositol-4,5-bisphosphate 3-kinase catalytic subunit alpha	
PIK3R1	chr5	6625	Phosphoinositide-3-kinase regulatory subunit 1	
PTEN	chr10	3974	Phosphatase and tensin homolog	
TAF1	chrX	11,840	TATA-box binding protein associated factor 1	
FGFR2	chr10	7522	Fibroblast growth factor receptor 2	RTK/RAS/MAPK signaling
KRAS	chr12	1615	KRAS proto-oncogene, GTPase	
MAP3K4	chr6	9345	Mitogen-activated protein kinase kinase kinase 4	
NRAS	chr1	1606	NRAS proto-oncogene, GTPase	
BCOR	chrX	8733	BCL6 corepressor	Diverse
CSMD3	chr8	26,363	CUB and sushi multiple domains 3	
CTCF	chr16	4977	CCCTC-binding factor	
FBXW7	chr4	5905	F-box and WD repeat domain containing 7	
FOXA2	chr20	2303	Forkhead box A2	
KLLN	chr10	1265	Killin, P53 regulated DNA replication inhibitor	
PGAP3	chr17	1170	Post-GPI attachment to proteins 3	
PRPF18	chr10	2835	Pre-MRNA processing factor 18	
RPL22	chr1	947	Ribosomal protein L22	
SCARNA11	chr12	867	Small Cajal body-specific RNA 11	
SIN3A	chr15	8292	SIN3 transcription regulator family member A	
SPOP	chr17	3542	Speckle type BTB/POZ protein	
TSPYL2	chrX	3192	TSPY like 2	
USP36	chr17	6645	Ubiquitin specific peptidase 36	

In table are reported gene symbol, chromosome localization (Chr.), gene target region analyzed in base pairs (bps), gene description, and gene-related functional pathway

Tris/EDTA buffer, pH 9. Before staining the sections, endogenous peroxidase was blocked. Samples were subjected to IHC for p53, PTEN, ARID1A, MSH6, and PMS2. Antibody, clone, source, and dilution are shown in Table 3. After incubation, the reaction was visualized with the EnVision FLEX Detection Kit (DAKO) using diaminobenzidine chromogen as a substrate. Sections were counterstained with hematoxylin. Appropriate

Table 3 Antibody, clone, source, and dilution

Antibody	Clone	Source	Dilution
p53	DO7	DAKO	RTU
ARID1A	EPR13501–73	DAKO	1/500
PTEN	6H2.1	DAKO	1/100
MSH6	EP49	DAKO	RTU
PMS2	EP51	DAKO	RTU

RTU, ready to use

negative controls were also tested. Scoring criteria for the five biomarkers were the following: p53 was scored as "mutated" pattern (strong staining in more than 80% of tumor cells or complete negative staining) versus "wild type" pattern; and PTEN, ARID1A, MSH6, and PMS2 were scored as positive (any staining) versus negative (absence of staining).

TCGA-based molecular classification by surrogate markers

Each sample was molecularly classified (Table 1) according to TCGA-based surrogate (*POLE* Sanger sequencing and immunohistochemical testing of p53, MSH-6, and PMS-2). Four categories were established: (1) microsatellite unstable (MSI) (hypermutated) class including cases with negative staining for MSH-6 or PMS-2, (2) serous-like category including cases with just p53 "mutated" IHC pattern, (3) NSMP class grouping tumors with no specific molecular profile, and (4) *POLE*-mutated category (ultramutated). Tumors with more than one surrogate marker (MSI and p53) were classified as double mutated. Tumors with *POLE* mutations were classified as *POLE*-mutated regardless of the presence of MSI or p53 "mutated" IHC pattern.

Statistical analysis

Absolute and relative (percentage) presence of mutations for each gene was computed in EEC and SC cases, computing the odds ratio (with small sample adjustment when no mutation was detected in EEC and/or SC cases) and its corresponding *p* value to assess the strength and significance of the association. To depict the ability of genes to discriminate between EEC and SC cases, two heatmaps were produced (one with all-altered genes and other with significant genes), using double hierarchical cluster analysis with Euclidean distance. All analyses were made using the open-source R statistical software (www.r-poject.org). Threshold for significance level was set at $\alpha = 0.05$.

Results

Mutation profile by targeted sequencing

Targeted sequencing analysis produced a mean of 2,270,521 reads, 97.64% of which mapped on reference genome version GRCh38/hg38 with high quality without PCR duplicates. Mean coverage depth was of 1563× per sample, being average depth and reads of normal and tumor samples similar.

After applying the previously described filters, our analysis identified a total of 164 somatic variants (Supplementary Table 1). Somatic variants were classified according to variant effect on transcripts as missense (62%), frameshift (24%), stop gained (9%), splice acceptor (1%), protein-altering (1%), and inframe deletions (4%). These variants were also classified depending on their pathogenicity degree: 51% of pathogenic variants (PV), 21% of likely pathogenic variants (LPV), 24% of variants of unknown significance (VUS), and 4% of likely benign or neutral variants (LBNV) (Fig. 1).

In the EEC group, we found a mean of 7.8 variants per sample (range 3 to 19), and in the SC, a mean of 2.6 variants per sample (range 1 to 5). Table 4 shows the genes more frequently altered in EEC and SC. No mutations were found in *ABCC9*, *CSDE1*, *KLLN*, *PGAP3*, *SCARNA11*, *SPOP*, *TSPYL2*, and *WRAP53* genes.

Recurrent mutations affecting protein domains in most frequently mutated genes were identified using the Mutation Mapper (www.cbioportal.org). This tool allowed us to locate mutations in protein domains according to Pfam database and thus, to assess the relevance of detected variants. Most likely mutational hotspots in *PTEN*, *TP53*, *PIK3CA*, and *ARID1A* genes are shown in Fig. 2. The 45% (10/22) of *PTEN*-detected variants were located in the C2 domain and 31.8% (7/22) in the DPSc domain, being R130 the most frequent hotspot (71.4%, 5/7). The 72.8% (16/22) of *PTEN* variants generated a truncated protein, and the 22% (5/22) of the remaining variants were missense. In the case of *TP53* gene, the 86% (13/15) of mutations occurred in the p53 DNA-binding domain. Unlike *PTEN*, 80% (12/15) of *TP53* mutations were missense and just two variants built a truncated protein (13%). Interestingly, we found a different mapping of *PIK3CA* mutations depending on tumor type. SC samples had *PIK3CA* gene mutations located at the end of exon 2 and at the beginning of exon 3. Instead, EEC group harbored *PIK3CA* variants widely distributed. These cases showed those typical exon 9 and 20 hotspots at 25% and 37% frequencies, respectively. For *ARID1A* gene, mutations were distributed throughout the entire gene, without finding any specific hotspot, 64.3% were truncating mutations and 35.7% were missense mutations.

KMT2B gene mutations were not mapped in known protein domains. The 57% were missense variants where L417P mutation represented 75% of them, and the remaining 43%

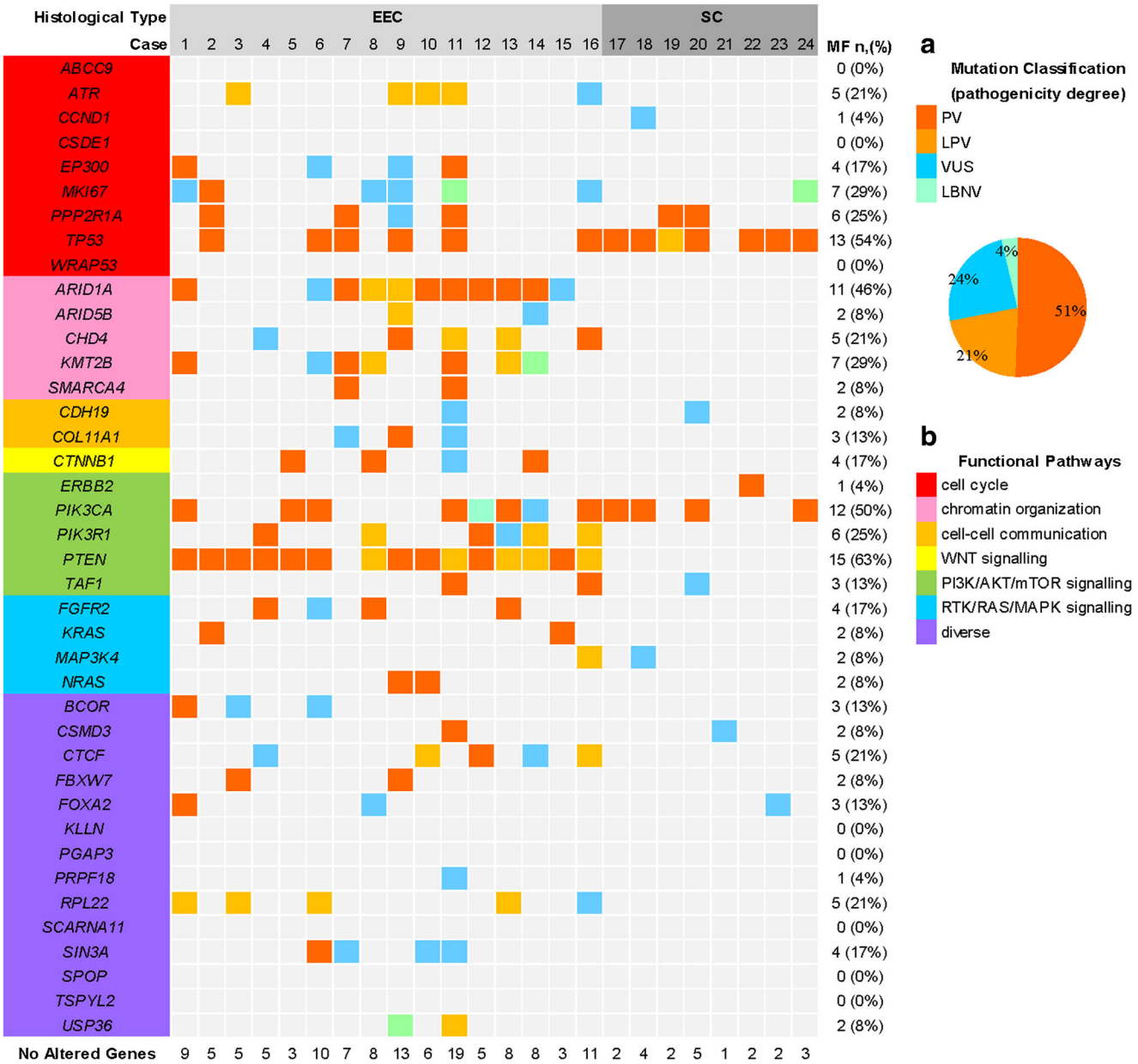

Fig. 1 Distribution of detected somatic mutations according to cases and analyzed genes. At the top of the *x*-axis, cases are grouped by histological type (EEC, endometrioid carcinomas; SC, serous carcinomas), and at the bottom, the number of altered genes per case is shown. At the right of the *y*-axis, mutation frequency (MF (*n* (%)) per gene is shown. Colored boxes were drawn to indicate: **a** The mutation classification according to pathogenicity degree: PV (pathogenic variants) in strong orange, LPV (likely pathogenic variants) in light orange, VUS (variants of unknown significance) in blue, and LBNV (likely benign or neutral variants) in green. Pie chart below shows somatic mutation percentage based on the pathogenicity degree classification; and to indicate: **b** Functional pathways associated to analyzed genes: cell cycle in red, chromatin organization in pink, cell-cell communication in light orange, Wnt signaling in yellow, PI3K/AKT/mTOR signaling in green, RTK/RAS/MAPK signaling in blue, and diverse in purple

corresponded to frameshift mutations. All mutations detected in *PPP2R1A* gene were missense; from them, P179R was the most observed (50%, 3/6). Cases with more than one mutation in the same gene were found for *PTEN*, *ARID1A*, *PIK3CA*, and *TP53*.

Most frequently altered genes in our sample set belong to the following signaling pathways: PI3K/AKT/mTOR including *PTEN* and *PIK3CA*, cell cycle including *TP53* and *PPP2R1A*, and chromatin organization with *ARID1A* and *KMT2B*.

According to TCGA reports [9], all five samples with *RPL22* mutation harbored p.Lys15ArgfsTer5 variant and four of them presented lack of microsatellite stability (MSI).

Histological classification by targeted sequencing

Mutational profile of the 24 tumors was concordant with histological typing in all cases. Most frequently mutated genes

Table 4 Absolute number (*n*) and mutation frequency (%) of altered genes in EEC and SC

Gene symbol	Mutated cases, *n* (%)		Odds ratio		*p* value
	EEC (16 cases)	SC (8 cases)	EEC vs SC	SC vs EEC	
*PTEN**	15 (93.75%)	0 (0%)	60.00		0.00001*
*ARID1A**	11 (68.75%)	0 (0%)	14.67		0.002*
*TP53**	6 (37.5%)	7 (87.5%)		9.62	0.03*
*KMT2B**	7 (43.75%)	0 (0%)	5.60		0.03*
PIK3R1	6 (37.5%)	0 (0%)	4.36		0.06
ATR	5 (31.25%)	0 (0%)	3.33		0.1
CHD4	5 (31.25%)	0 (0%)	3.33		0.1
CTCF	5 (31.25%)	0 (0%)	3.33		0.1
RPL22	5 (31.25%)	0 (0%)	3.33		0.1
CTNNB1	4 (25%)	0 (0%)	2.46		0.17
EP300	4 (25%)	0 (0%)	2.46		0.17
FGFR2	4 (25%)	0 (0%)	2.46		0.17
SIN3A	4 (25%)	0 (0%)	2.46		0.17
MKI67	6 (37.5%)	1 (12.5%)	3.66		0.25
BCOR	3 (18.75%)	0 (0%)	1.71		0.28
COL11A1	3 (18.75%)	0 (0%)	1.71		0.28
CCND1	0 (0%)	1 (12.5%)		2.00	0.33
ERBB2	0 (0%)	1 (12.5%)		2.00	0.33
FBXW7	2 (12.5%)	0 (0%)	1.07		0.43
KRAS	2 (12.5%)	0 (0%)	1.07		0.43
NRAS	2 (12.5%)	0 (0%)	1.07		0.43
SMARCA4	2 (12.5%)	0 (0%)	1.07		0.43
USP36	2 (12.5%)	0 (0%)	1.07		0.43
CDH19	1 (6.25%)	1 (12.5%)		2.07	0.67
CSMD3	1 (6.25%)	1 (12.5%)		2.07	0.67
MAP3K4	1 (6.25%)	1 (12.5%)		2.07	0.67
ARID5B	1 (6.25%)	0 (0%)	1.01		0.67
PRPF18	1 (6.25%)	0 (0%)	1.01		0.67
FOXA2	3 (18.75%)	1 (12.5%)	1.48	0.67	0.76
TAF1	2 (12.5%)	1 (12.5%)		1.05	0.97
PPP2R1A	4 (25%)	2 (25%)	1.00	1.00	0.98
PIK3CA	8 (50%)	4 (50%)	1.00	1.00	1

*Indicate genes associated to tumor type ($p < 0.05$)

were *PTEN* (93.7%), *ARID1A* (68.7%), *PIK3CA* (50%), and *KMT2B* (43.7%) for EEC, and *TP53* (87.5%), *PIK3CA* (50%), and *PPP2R1A* (25%) for SC (Table 4).

Our panel allowed correct tumor classification in the two categories (EEC, SC). Tumor type was found to be associated with mutations in four different genes ($p < 0.05$), being *PTEN* (OR = 60, $p = 0.00001$), *ARID1A* (OR = 14.67, $p = 0.002$), and *KMT2B* (OR = 5.6, $p = 0.03$) associated with EEC type, and *TP53* (OR = 9.62, p = 0.03) with SC type (Table 4). Coexistence of mutations in *PTEN*, *ARID1A*, and *KMT2B* was diagnostic of EEC. On the other hand, absence of *PTEN*, *ARID1A*, and *KMT2B* in the presence of *TP53* mutation was diagnostic of SC. *TP53* and *PIK3CA* mutations were present in both tumor types.

Figure 3 shows the heatmaps depicting the presence of mutations in all 32 altered genes and those statistically significant, showing that cases with the same tumor type (EEC or SC) are classified correctly.

Sanger validation and *POLE* mutation analysis

Sanger sequencing analysis allowed the correct identification of the same variants found by targeted sequencing for *TP53*, *PTEN*, and *ARID1A* genes (Table 5).

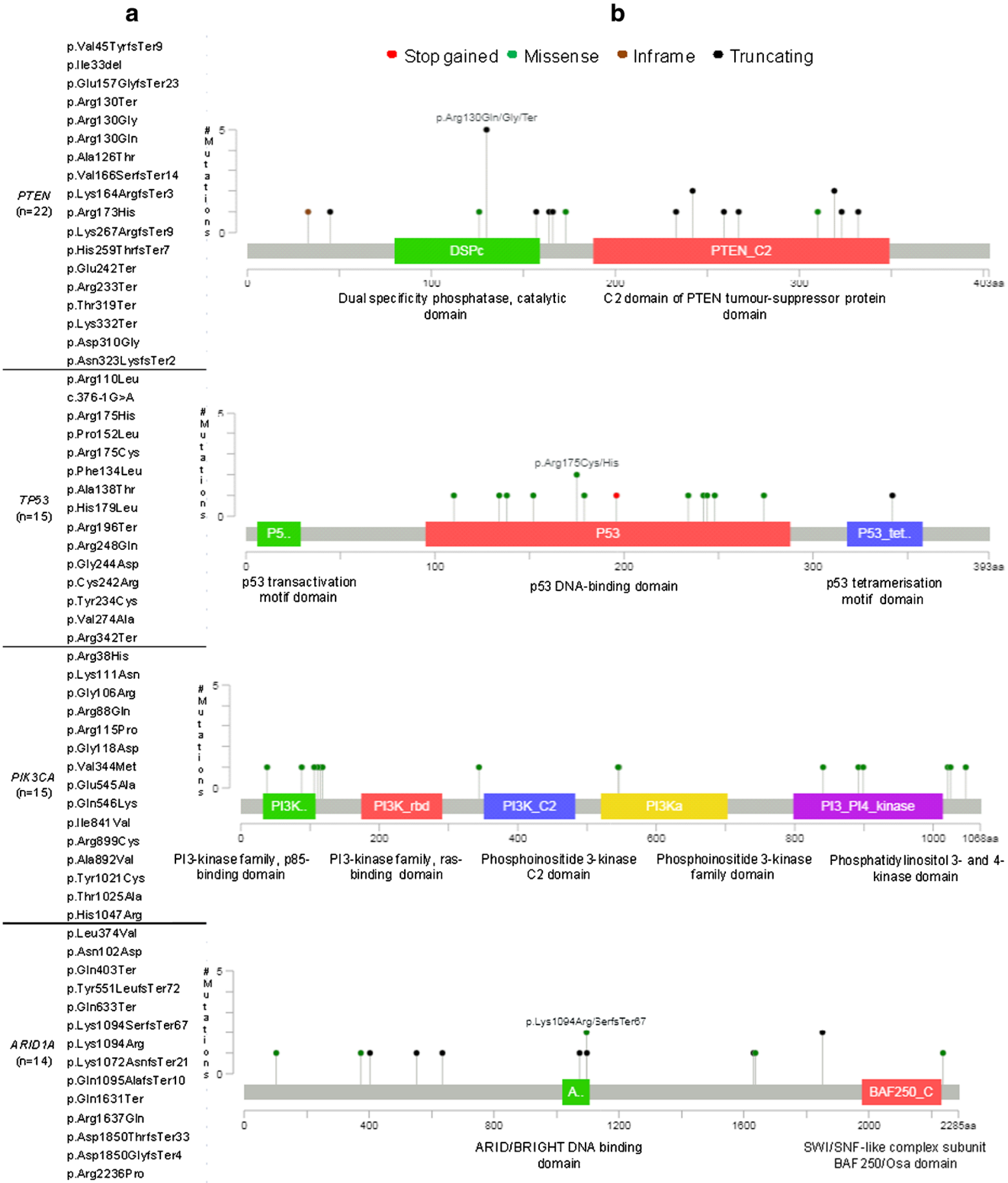

Fig. 2 **a** List of somatic mutations identified in *PTEN*, *TP53*, *PIK3CA*, and *ARID1A* genes. **b** Lollipop plots mapping detected somatic mutations on respective linear protein and its Pfam domains (Mutation Mapper tool). The *y*-axis indicates the number of mutations, and the *x*-axis represents the protein sequence with numbers below indicating amino acid sequence positions

Additionally, *POLE* mutation analysis by Sanger sequencing demonstrated *POLE* wild-type sequence in all but one of the cases, which showed the POLE gene variant p.Y458N.

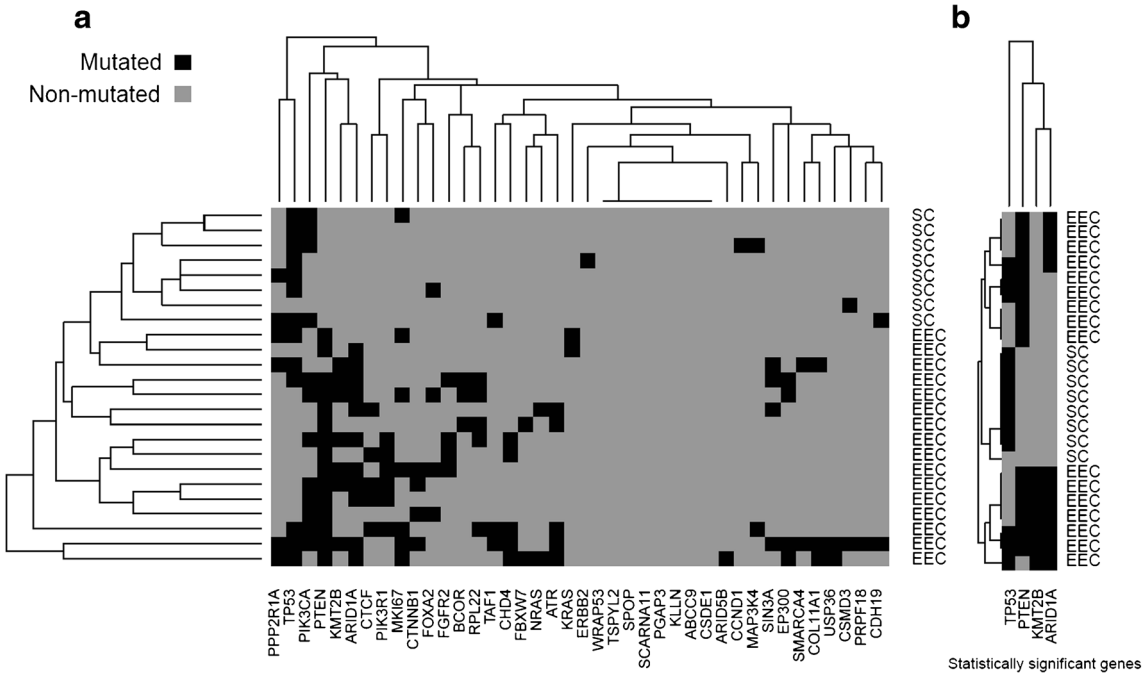

Fig. 3 **a** Heatmap depicting presence of mutations in all 32 altered genes (columns) for EEC and SC cases (rows). **b** Heatmap showing the presence of mutations in four statistically significant genes (columns) for EEC and SC cases (rows). Note that heatmaps were created using a double hierarchical cluster analysis with a Euclidean distance

Immunohistochemical validation

Immunohistochemical validation was performed for *TP53*, *PTEN*, and *ARID1A* genes (Table 5). Moreover, immunostaining for MSH6 and PMS2 was done. Correlation between immunohistochemistry and sequencing analysis was obtained in the vast majority of cases. Twelve of the 13 *TP53* gene-mutated tumors resulted in a "mutated" p53 IHC pattern. PTEN negative staining was seen in 13 of 15 mutated tumors. Negative staining for ARID1A was observed in 10 of the 12 *ARID1A*-mutated tumors. Negative immunostaining for MSH6 was obtained in 2 cases, while negativity for PMS2 was detected in 7 cases. Overall mismatch repair deficiency was detected in 9 cases; all of them are EEC; and in 2 cases, mismatch repair deficiency coexisted with p53 "mutated" IHC pattern. Cases with mismatch repair deficiency had a range of 7 to 19 mutations (mean 10, median 9). Cases without mismatch repair deficiency had a range of 1 to 6 mutations (mean 3.7, median 4). The only one *POLE*-mutated (case 11) was an EEC grade 3 tumor which showed negative staining for PMS2 as well as the highest number of mutations (19) including *TP53*, *PTEN*, and *ARID1A* genes.

Discussion

Histological type is considered an important biologic predictor in EC [1–3]. EEC grades 1 and 2 tumors (EEC 1 and 2) are usually associated with a favorable outcome, while prognosis for SC is worse. EEC grade 3 (EEC 3) is a heterogeneous group of tumors, with an adverse prognosis subgroup [10]. Recurrence occurs in about 20% of EEC and 50% of SC. SC and EEC 3 tumors had been compared using Surveillance, Epidemiology, and End Results (SEER) program data from 1988 to 2001. They represented 10% and 15% of EC, respectively, but accounted for 39% and 27% of endometrial cancer deaths, respectively [11]. Moreover, assessment of histological type determines the extent of initial surgical procedure and subsequent use of adjuvant therapy [4]. Although there is moderate to excellent (0.62–0.87) reproducibility in histological typing, inter-observer agreement is worse in high-grade tumors [8].

EEC 1 and 2 are usually composed of cells arranged in a glandular pattern of growth which is reminiscent of that of the proliferative endometrium, while EEC 3 has a predominant solid arrangement, and serous carcinomas have a complex architectural pattern with papillae and cellular budding [4]. However, SC with prominent glandular pattern is frequently mistaken as EEC 1 and 2; on the other hand, EEC with papillary pattern is sometimes interpreted as SC [4–7]. Differential diagnosis is difficult in a subset of cases.

The Cancer Genome Atlas (TCGA) has provided an integrated genomic characterization of EC and has proposed a new molecular classification in four groups of tumors [9]. Group 1 encompass EEC with 7% of somatic inactivating mutations in *POLE* exonuclease (ultramutated), associated with good prognosis. They have very high mutation rate (232 × 106 mutations/Mb) and are characterized by mutations

Table 5 *ARID1A*, *PTEN*, and *TP53* mutation validation analysis by the Sanger sequencing and immunohistochemistry

	ARID1A			*PTEN*			*TP53*		
Case	Targeted	Sanger	IHC	Targeted	Sanger	IHC	Targeted	Sanger	IHC
1	K1072NfsTer21 R2236P	K1072NfsTer21 R2236P	NS	K332*	K332*	NS	WT	ND	"WT"P
2	WT	ND	PS	D310G	D310G	NS	R175H	R175H	"M"P
3	WT	ND	PS	R233*	R233*	NS	WT	ND	"WT"P
4	WT	ND	PS	R130*	R130*	NS	WT	ND	"WT"P
5	WT	ND	PS	R130G	R130G	PS	WT	ND	"WT"P
6	K1094SfsTer67	K1094SfsTer67	NS	A126T K267RfsTer9	A126T K267RfsTer9	NS	R248Q P152L	R248Q P152L	"M"P
7	R1637Q	R1637Q	PS	WT	ND	PS	R175C	R175C	"M"P
8	Y551LfsTer72	Y551LfsTer72	NS	T319*	T319*	NS	WT	ND	"WT"P
9	D1850TfsTer4	D1850TfsTer4	NS	R130* R173H	R130* R173H	NS	G244D	G244D	"WT"P
10	Q633*	ND	NS	V45YfsTer9 H259TfsTer7	V45YfsTer9 H259TfsTer7	NS	WT	ND	"WT"P
11	K1094R D1850GfsTer4	K1094R D1850GfsTer4	PS	E157GfsTer23 N323KfsTer2	E157GfsTer23 N323KfsTer2	NS	F134 L	F134 L	"M"P
12	Q403*	Q403*	NS	R130* R130Q	R130* R130Q	PS	WT	ND	"WT"P
13	Q1095AfsTer10	Q1095AfsTer10	NS	E242*	E242*	NS	WT	ND	"WT"P
14	Q1631*	Q1631*	NS	K164RfsTer3	ND	NS	WT	ND	"WT"P
15	N102D L374 V	ND	NS	E242*	E242*	NS	WT	ND	"WT"P
16	P373R[#] Q372SfsTer19[#]	ND	NS	I33del T319*	I33del T319*	NS	A138T	A138T	"M"P
17	WT	ND	PS	WT	ND	PS	R196*	R196*	"M"P
18	WT	ND	PS	WT	ND	PS	V274A	V274A	"M"P
19	WT	ND	PS	WT	ND	PS	R342*	R342*	"M"P
20	WT	ND	PS	WT	ND	PS	C242R	C242R	"M"P
21	WT	ND	PS	WT	ND	NV	WT	ND	"WT"P
22	WT	ND	PS	WT	ND	NV	Splice acceptor c.376-1G > A	Splice acceptor c.376-1G > A	"M"P
23	WT	ND	PS	WT	ND	NS	H179L R110L	H179L R110L	"M"P
24	WT	ND	PS	WT	ND	NV	Y234C	Y234C	"M"P

[#] Indicate ARID1A mutations below the 100× tumor depth filter (case 16 tumor depth = 4); *Indicate that the consequence of the mutation at protein level is a termination codon. *NS*, negative staining; *PS*, positive staining; *NV*, not valuable; "*WT*"*P*, "wild type" pattern; "*M*"*P*, "mutated" pattern; *ND*, not done

in *PTEN*, *PIK3CA*, *PIK3R1*, *FBXW7*, *ARID1A*, *KRAS*, and *ARID5B*. Group 2 includes EEC with microsatellite instability (hypermutated), frequently associated with *MLH-1* promoter hypermethylation (28%). They have high mutation rate (18 × 106 mutations/Mb) and show mutations in *PTEN*, *RPL22*, *KRAS*, *PIK3CA*, *PIK3R1*, and *ARID1A*. Group 3 tumors include EEC with low copy-number alterations (39%), also called EC with no specific molecular profile. They show low mutation rate (2.9 × 106 mutations/Mb) including mutations in *PTEN*, *CTNNB1*, *PIK3CA*, *PIK3R1*, and *ARID1A*. Group 2 and group 3 both show similar progression-free survival rates. Finally, group 4 called serous-like or copy-number high (26%) show frequent *TP53* mutations and worse prognosis and is predominantly composed of most (but not all) SC, but also some EEC (many EEC 3, but also some EEC 1 and 2). They have low mutation rate (2.3 × 106 mutations/Mb), with frequent mutations in *TP53*, *PPP2R1A*, and *PIK3CA* and show chromosomal instability, with recurrent gene amplifications for *MYC*, *ERBB2*, *CCNE1*, *FGFR3*, and *SOX17*.

Although molecular classification is already important to predict prognosis, histological typing remains the gold standard for tumor stratification. Combination of POLE mutational analysis and IHC testing of p53 and mismatch repair proteins (PMS-2 and MSH-6) has been proposed as a surrogate strategy to classify EC into the four TCGA groups [10, 12, 13]. There is some controversy regarding the possibility that the molecular classification would replace the traditional histological typing in daily practice. The main reason in favor of

molecular classification is the poor inter-observer agreement in histological typing in a subset of EC. Incorporation of TCGA-based surrogate classification into clinical practice may carry important advantages. Identification of *POLE*-mutated and serous-like/high copy-number tumors may lead to a much better clinical management of these patients. Molecular classification still needs further validation to solve some unresolved issues. For example, a subset of *POLE*-mutated and microsatellite unstable tumors show also p53 "mutated" IHC pattern and *TP53* mutation ("double positive"). These cases raise the differential diagnosis with serous-like/high copy-number EC. Moreover, the current TCGA-based surrogate approaches are not perfect. Nowadays, p53 immunostaining is used to identify the serous-like or copy-number high group. However, the correlation between p53 immunostaining and *TP53* mutation is not perfect. Using p53 immunostaining as a surrogate, *TP53* wild-type serous-like tumors are incorrectly classified as EC with no specific molecular profile. Finally, there are some preliminary evidences suggesting that, even in the serous-like group, the pattern of metastasis may be different, depending on histological type. The most probable scenario for the future is the coexistence of these classification systems, traditional histological typing, and molecular classification [14]. Based on that idea, it remains interesting to improve the tools for distinguishing EEC from SC.

Several IHC biomarkers have been shown to have a differential immunostaining pattern in EEC, including EEC 3, as opposed to SC. Some of these IHC markers were previously found to be differentially expressed between EEC and SC by cDNA analysis [15–17]. They include estrogen receptor, PTEN, HER2, claudins 3 and 4, Nrf2, p53, p16, FOLR-1, HMGA-2, cyclin E, IMP2, and IMP3 [18–23]. Several authors have attempted the use of panels of antibodies to help in diagnosis and prognosis [24–26]. There is no single or antibody combination profile which can discriminate between EEC and SC due to a degree of overlap. However, in daily practice, p53, p16, IMP2, and IMP3 are helpful tools.

Molecular alterations involved in the development of EEC are different from those of SC [27, 28]. EEC shows microsatellite instability, as well as mutations in *PTEN*, *KRAS*, and *CTNNB1* genes whereas SC exhibits alterations of *TP53*, widespread loss of heterozygosity, as reflected by chromosomal instability as well as other molecular alterations (STK15, p16, E-cadherin, and C-erbB2). *PIK3CA* and *ARID1A* mutations have been identified in both tumor types. Recently [9], TCGA study confirmed a different mutational profile between EEC and SC. The most frequently mutated genes in EEC were *PTEN* (77%), *PIK3CA* (53%), *PIK3R1* (37%), *CTNNB1* (36%), *ARID1A* (35%), *KRAS* (24%), *CTCF* (20%), *RPL22* (12%), *TP53* (11%), *FGFR2* (11%), and *ARID5B* (11%). The most frequently mutated genes in SC were *TP53* (90.7%), *PIK3CA* (41.9%), *FBXW7* (30.2%), *PPP2R1A* (36.6%), *CHD4* (16.3%), *CSMD3* (11.6%), and *COL11A1* (11.6%) [9].

Several authors have used targeting sequencing in EC. Chang et al. [29] assessed ten cases of EC using the Nimble Gen Comprehensive Cancer Panel that includes 578 cancer-related genes. This survey revealed 120 variants in 99 genes, 21 of which were included in the Oncomine Cancer Research Panel. Mass spectrometric–based mutation analysis was also used in several studies [30]. Lately, a panel of cancer-related genes was used to identify increased mutational load in EC with deficient DNA mismatch repair [31]. McConechy et al. [32] performed target enrichment sequencing on 393 EC, by sequencing nine genes (*ARID1A*, *PPP2R1A*, *PTEN*, *PIK3CA*, *KRAS*, *CTNNB1*, *TP53*, *BRAF*, and *PPP2R5C*) and suggest that this nine-gene panel may be useful as an adjunct to the morphological classification of EC. The authors found that majority of microscopical diagnoses were concordant with the identified genotype. However they noticed a subset of genotype-incompatible diagnoses [33].

In the present study, we used targeting sequencing as a tool for assessing histological typing. We decide to use a customized gene panel that included most frequently mutated genes in EEC and SC, according to TCGA. This unique panel has never been tested before in the literature for histological typing in EC. In this proof of concept study, we selected 24 well-characterized cases at microscopical level which included the four TCGA molecular groups. Three cases were especially interesting; case 9 was a MSI with p53 "wild type" IHC pattern but with a TP53 detected mutation; case 11 was a *POLE*-mutated tumor that showed a p53 "mutated" IHC pattern; and case 21 was a SC that had a "wild type" p53 IHC pattern but otherwise typical features of SC. Remaining cases were more or less classical EEC and SC.

The targeted sequencing analysis produced a mean of 2,270,521 reads. We identified a total of 164 somatic variants (102 missense, 39 frameshift, 15 stop gained, 1 splice acceptor, 1 protein altering, and 6 inframe deletions), and 72% of them were either pathogenic or likely pathogenic variants. The mutational profile of the 24 tumors was concordant with the pathologic diagnosis in all cases. Most mutated genes in the 16 EEC cases were *PTEN* (93.7%), *ARID1A* (68.7%), *PIK3CA* (50%), and *KMT2B* (43.7%) whereas the 8 SC tumors showed mutations in *TP53* (87.5%), *PIK3CA* (50%), and *PPP2R1A* (25%). Our customized gene panel allowed correct classification of all tumors in the two categories. Coexistence of mutations in *PTEN*, *ARID1A*, and *KMT2B* genes was diagnostic of EEC. On the other hand, absence of *PTEN*, *ARID1A*, and *KMT2B* in the presence of *TP53* mutation was diagnostic of SC. *TP53* and *PIK3CA* mutations were present in both tumor types.

Targeted sequencing results were validated by the Sanger sequencing and immunohistochemistry for *TP53*, *PTEN*, and *ARID1A* genes, showing a nice correlation between validation techniques. In general, *TP53* gene

mutations were associated with a "mutated" p53 IHC pattern (only one *TP53* mutated tumor showed "wild type" p53 pattern by IHC). Cases with *ARID1A* and *PTEN* gene mutations exhibited concordance with negative immunostaining in 83% and 86%, respectively. Mismatch repair deficiency, by IHC, was restricted to EEC cases. Interestingly, there was a nice correlation between the presence of mismatch repair deficiency, as assessed by IHC for MSH6 and PMS2, and the number of mutations, although it is clear that our approach is not the correct tool to assess tumor mutation load. A *POLE*-mutated, EEC grade 3 showed negative expression of MSH6, "mutated" IHC pattern for p53, negative PTEN staining, and the highest number of mutations, including one in *TP53* and one in *PTEN* (case 11). A high-grade EC double mutated (case 6) was correctly classified as EEC 3 by targeted sequencing (Fig. 4). The series included a SC that had a "wild type" IHC p53 staining pattern, but otherwise typical microscopical features of SC (case 21). Targeted sequencing correctly classified the tumors as SC, and confirmed the lack of *TP53* mutations. This case illustrates the fact that there is a subset of SC (9% according to TCGA) that does not show either *TP53* mutations or "mutated" p53 IHC pattern. Interestingly, this case would be misclassified as EC with no specific molecular profile, based on the "wild type" IHC pattern for p53 by the surrogate TCGA approach, while targeted sequencing confirms that the correct diagnosis is SC. Exome sequencing of this case (data not shown) confirmed a high number of copy-number alterations and, thus, the tumor was a serous-like EC. There was an additional tumor (case 9) that was erroneously classified by the TCGA-based surrogate in the group of microsatellite unstable tumors, because of negative mismatch repair and "wild type" p53 IHC pattern. It showed a *TP53* mutation, either by targeted and Sanger

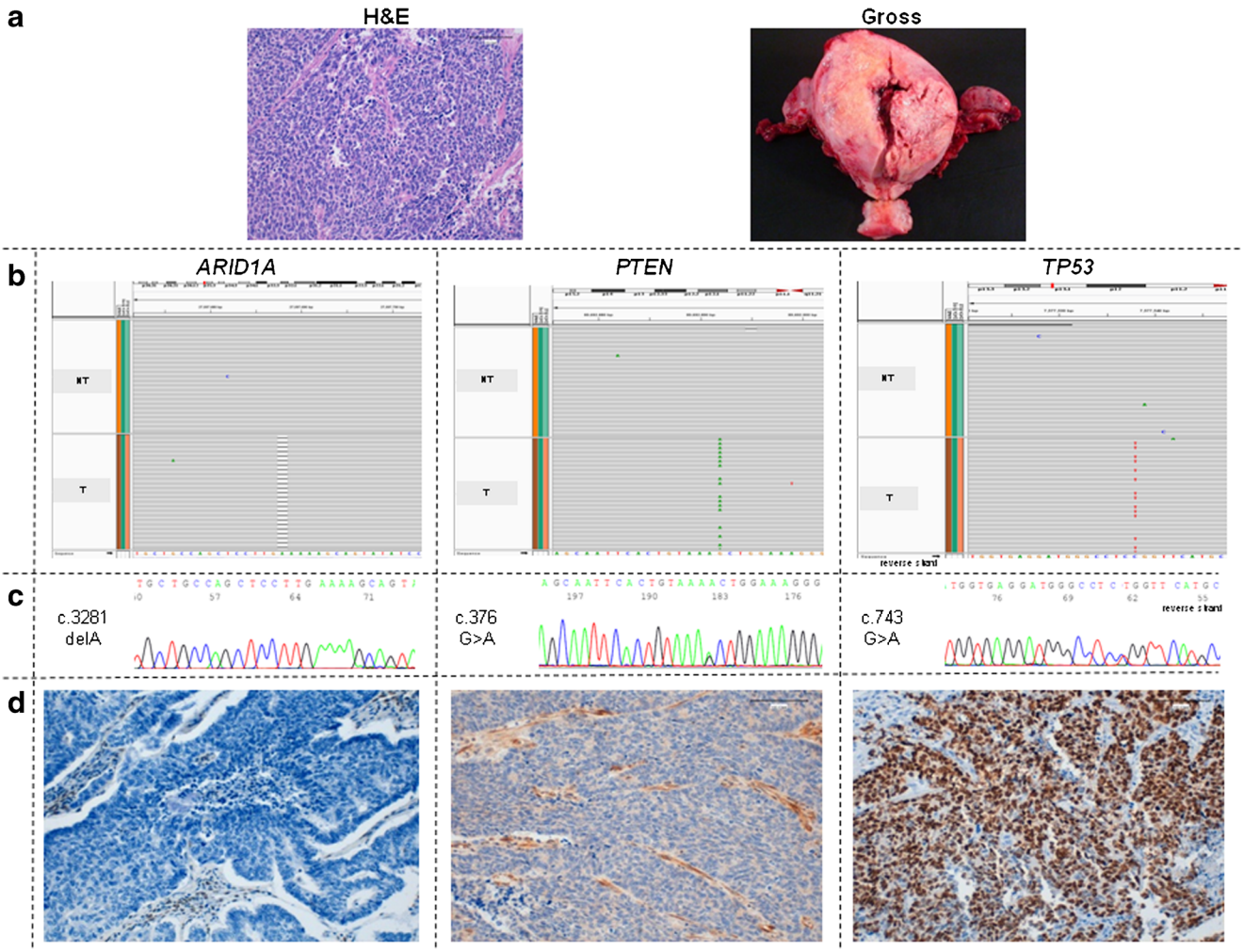

Fig. 4 Photomic depiction to illustrate integration of anatomic and molecular pathology of a FIGO EEC grade 3 (case 6). Microscopic (× 20) and gross appearance (**a**); *ARID1A* (c.3281delA, p.K1094SfsTer67), *PTEN* (c.376G > A, p.A126T), and *TP53* (c.743 G > A, R248Q) mutations detected by targeted sequencing and visualized through IGV (Integrative Genomic Viewer) tool (**b**) and detected by the Sanger sequencing (**c**); ARID1A, PTEN, and TP53 immunohistochemistry (× 20) (**d**)

sequencing demonstrating that indeed was a really double mutated tumor. Overall, targeted sequencing analysis showed that TCGA-based surrogate misclassified 2 of the 24 tumors in this series of cases.

In summary, this proof of concept study demonstrates the suitability of targeted sequencing with a customized endometrial cancer gene panel as an additional tool for confirming histological typing. The strategy seems interesting as a tool to classify tumors with unusual microscopical findings, as well as tumors with unexpected IHC features, such as SC without *TP53* alterations, as illustrated in one case of this series. Nevertheless, further studies with a larger series containing consecutive cases are required to validate this approach in equivocal cases with combined or mixed features between EEC and SC.

Author's contribution Dolors Cuevas: collected samples, collected clinical patient data, performed experiments, analyzed data, participated in study design, and wrote, edited, and reviewed the manuscript.

Joan Valls: performed statistical analysis and wrote part of the manuscript.

Sònia Gatius: collected clinical and histological patient data, assisted in histopathological examinations, and wrote part of the manuscript.

Berta Roman-Canal: reviewed the manuscript.

Elena Estaran: assisted in histopathological examinations.

Eduard Dorca: assisted in histopathological examinations.

Maria Santacana: performed immunohistochemical experiments and wrote part of the manuscript.

Marta Vaquero: assisted in carrying out experiments and reviewed the manuscript.

Ana Velasco: participated in study design, assisted in carrying out experiments, and reviewed the manuscript.

Núria Eritja: assisted in data collection and reviewed the manuscript.

Xavier Matias-Guiu: conceived and designed the study and wrote, edited, and reviewed the manuscript.

Funding The research team was supported by grants from the ISCIII (PI16/00692, CB16/12/00231) and Generalitat de Catalunya 2014SGR138. Tumor samples were obtained with the support of Xarxa Catalana de Bancs de Tumors and Plataforma de Biobancos ISCIII (PT 17/0015/0027).

Compliance with ethical standards

Conflict of interest The authors declare that they have no conflict of interest.

References

1. Prat J (2004) Prognostic parameters of endometrial carcinoma. Hum Pathol 35:649–662
2. Matias-Guiu X, Davidson B (2014) Prognostic biomarkers in endometrial and ovarian carcinoma. Virchows Arch 464:315–331
3. Salvesen HB, Haldorsen IS, Trovik J (2012) Markers for individualised therapy in endometrial carcinoma. Lancet Oncol 13:e353–e361
4. Clarke BA, Gilks CB (2010) Endometrial carcinoma: controversies in histopathological assessment of grade and tumor cell type. J Clin Pathol 63:410–415
5. Bartosch C, Manuel LJ, Oliva E (2011) Endometrial carcinomas: a review emphasizing overlapping and distinctive morphological and immunohistochemical features. Adv Anat Pathol 18:415–437
6. Soslow RA (2013) High-grade endometrial carcinomas - strategies for typing. Histopathology 62:89–110
7. Garg K, Soslow RA (2012) Strategies for distinguishing low-grade endometrioid and serous carcinomas of endometrium. Adv Anat Pathol 19:1–10
8. Gilks CB, Oliva E, Soslow RA (2013) Poor interobserver reproducibility in the diagnosis of high-grade endometrial carcinoma. Am J Surg Pathol 37:874–881
9. Cancer Genome Atlas Research Network (2013) Integrated genomic characterization of endometrial carcinoma. Nature 497:67–73
10. Bosse T, Nout RA, McAlpine JN, McConechy MK, Britton H, Hussein YR, Gonzalez C, Ganesan R, Steele JC, Harrison BT, Oliva E, Vidal A, Matias-Guiu X, Abu-Rustum NR, Levine DA, Gilks CB, Soslow RA (2018) Molecular classification of grade 3 endometrioid endometrial cancers identifies distinct prognostic subgroups. Am J Surg Pathol 42:561–568
11. Hamilton CA, Cheung MK, Osann K, Chen L, Teng NN, Longacre TA, Powell MA, Hendrickson MR, Kapp DS, Chan JK (2006) Uterine papillary serous and clear cell carcinomas predict for poorer survival compared to grade 3 endometrioid corpus cancers. Br J Cancer 94:642–646
12. Talhouk A, McConechy MK, Leung S, Li-Chang HH, Kwon JS, Melnyk N, Yang W, Senz J, Boyd N, Karnezis AN, Huntsman DG, Gilks CB, McAlpine JN (2015) A clinically applicable molecular-based classification for endometrial cancers. Br J Cancer 113:299–310
13. Stelloo E, Nout RA, Osse EM, Jürgenliemk-Schulz IJ, Jobsen JJ, Lutgens LC, van der Steen-Banasik EM, Nijman HW, Putter H, Bosse T, Creutzberg CL, Smit VT (2016) Improved risk assessment by integrating molecular and clinicopathological factors in early-stage endometrial cancer-combined analysis of the PORTEC cohorts. Clin Cancer Res 22:4215–4224
14. Piulats JM, Guerra E, Gil-Martín M, Roman-Canal B, Gatius S, Sanz-Pamplona R, Velasco A, Vidal A, Matias-Guiu X (2017) Molecular approaches for classifying endometrial carcinoma. Gynecol Oncol 145:200–207
15. Moreno-Bueno G, Sanchez-Estevez C, Cassia R, Rodriguez-Perales S, Diaz-Uriarte R, Dominguez O, Hardisson D, Andujar M, Prat J, Matias-Guiu X, Cigudosa JC, Palacios J (2003) Differential gene expression profile in endometrioid and nonendometrioid endometrial carcinoma: STK15 is frequently overexpressed and amplified in nonendometrioid carcinomas. Cancer Res 63:5697–5702
16. Risinger JI, Maxwell GL, Chandramouli GV, Jazaeri A, Aprelikova O, Patterson T, Berchuck A, Barrett JC (2003) Microarray analysis reveals distinct gene expression profiles among different histologic types of endometrial cancer. Cancer Res 63:6–11
17. Alvarez T, Miller E, Duska L, Oliva E (2012) Molecular profile of grade 3 endometrioid endometrial carcinoma: is it a type I or type II endometrial carcinoma? Am J Surg Pathol 36:753–761
18. Wik E, Raeder MB, Krakstad C, Trovik J, Birkeland E, Hoivik EA, Mjos S, Werner HM, Mannelqvist M, Stefansson IM, Oyan AM, Kalland KH, Akslen LA, Salvesen HB (2013) Lack of estrogen receptor-alpha is associated with epithelial-mesenchymal transition and PI3K alterations in endometrial carcinoma. Clin Cancer Res 19:1094–1105

19. Morrison C, Zanagnolo V, Ramirez N, Cohn DE, Kelbick N, Copeland L, Maxwell GL, Fowler JM (2006) HER-2 is an independent prognostic factor in endometrial cancer: association with outcome in a large cohort of surgically staged patients. J Clin Oncol 24:2376–2385
20. Chen N, Yi X, Abushahin N, Pang S, Zhang D, Kong B, Zheng W (2010) Nrf2 expression in endometrial serous carcinomas and its precancers. Int J Clin Exp Pathol 4:85–96
21. Alkushi A, Lim P, Coldman A, Huntsman D, Miller D, Gilks CB (2004) Interpretation of p53 immunoreactivity in endometrial carcinoma: establishing a clinically relevant cut-off level. Int J Gynecol Pathol 23:129–137
22. Yemelyanova A, Ji H, Shih I, Wang TL, Wu LS, Ronnett BM (2009) Utility of p16 expression for distinction of uterine serous carcinomas from endometrial endometrioid and endocervical adenocarcinomas: immunohistochemical analysis of 201 cases. Am J Surg Pathol 33:1504–1514
23. McCluggage WG, Connolly LE, McBride HA, Kalloger S, Gilks CB (2012) HMGA2 is commonly expressed in uterine serous carcinomas and is a useful adjunct to diagnosis. Histopathology 60: 547–553
24. Alkushi A, Clarke BA, Akbari M, Makretsov N, Lim P, Miller D, Magliocco A, Coldman A, van de Rijn M, Huntsman D (2007) Identification of prognostically relevant and reproducible subsets of endometrial adenocarcinoma based on clustering analysis of immunostaining data. Mod Pathol 20:1156–1165
25. Reid-Nicholson M, Iyengar P, Hummer AJ, Linkov I, Asher M, Soslow RA (2006) Immunophenotypic diversity of endometrial adenocarcinomas: implications for differential diagnosis. Mod Pathol 19:1091–1100
26. Santacana M, Maiques O, Valls J, Gatius S, Abó AI, López-García MÁ, Mota A, Reventós J, Moreno-Bueno G, Palacios J, Bartosch C, Dolcet X, Matias-Guiu X (2014) A 9-protein biomarker molecular signature for predicting histologic type in endometrial carcinoma by immunohistochemistry. Hum Pathol 45:2394–2403
27. Yeramian A, Moreno-Bueno G, Dolcet X, Catasus L, Abal M, Colas E, Reventos J, Palacios J, Prat J, Matias-Guiu X (2013) Endometrial carcinoma: molecular alterations involved in tumors development and progression. Oncogene 32:403–413
28. Llobet D, Pallares J, Yeramian A, Santacana M, Eritja N, Velasco A, Dolcet X, Matias-Guiu X (2009) Molecular pathology of endometrial carcinoma: practical aspects from the diagnostic and therapeutic viewpoints. J Clin Pathol 62:777–785
29. Chang YS, Huang HD, Yeh KT, Chang JG (2016) Genetic alterations in endometrial cancer by targeted next-generation sequencing. Exp Mol Pathol 100:8–12
30. Krakstad C, Birkeland E, Seidel D, Kusonmano K, Petersen K, Mjøs S, Hoivik EA, Wik E, Halle MK, Øyan AM, Kalland KH, Werner HM, Trovik J, Salvesen H (2012) High-throughput mutation profiling of primary and metastatic endometrial cancers identifies KRAS, FGFR2 and PIK3CA to be frequently mutated. PLoS One 7:e52795
31. Lee PJ; McNulty S; Duncavage EJ; Heusel JW; Hagemann IS (2018) Clinical targeted next-generation sequencing shows increased mutational load in endometrioid-type endometrial adenocarcinoma with deficient DNA mismatch repair. Int J Gynecol Pathol 37:581–589
32. McConechy MK, Ding J, Cheang MC, Wiegand KC, Senz J, Tone AA, Yang W, Prentice LM, Tse K, Zeng T (2012) Use of mutation profiles to refine the classification of endometrial carcinomas. J Pathol 228:20–30
33. Hoang LN, McConechy MK, Köbel M, Han G, Rouzbahman M, Davidson B, Irving J, Ali RH, Leung S, McAlpine JN, Oliva E, Nucci MR, Soslow RA, Huntsman DG, Gilks CB, Lee CH (2013) Histotype-genotype correlation in 36 high-grade endometrial carcinomas. Am J Surg Pathol 37:1421–1423